



## Synthesis and electronic properties of *meso*-furyl boron dipyrromethenes

Tamanna K. Khan<sup>a</sup>, Sunit K. Jana<sup>a</sup>, M. Rajeswara Rao<sup>a</sup>, Mushtaque S. Shaikh<sup>b</sup>, M. Ravikanth<sup>a,\*</sup>

<sup>a</sup>Department of Chemistry, Indian Institute of Technology, Powai, Mumbai 400076, India

<sup>b</sup>Department of Pharmaceutical Chemistry, Bombay College of Pharmacy, Santacruz (E), Mumbai 400098, India

### ARTICLE INFO

#### Article history:

Received 2 March 2011

Received in revised form 11 October 2011

Accepted 8 November 2011

Available online 19 November 2011

#### Keywords:

*Meso*-furyl boron dipyrromethene

Hydrogen bonding

Dihedral angle

Stoke's shift

Easier reductions

### ABSTRACT

Four *meso*-furyl boron-dipyrromethenes (BODIPYs) were synthesized and characterized. The X-ray structures solved for three *meso*-furyl BODIPYs indicated the presence of an intramolecular hydrogen bond between *meso*-furyl 'O' and 'H' of boron-dipyrromethene core resulting in decrease of dihedral angle between the *meso*-furyl group and boron-dipyrromethene core leading to better electronic interaction. However, the hydrogen bonding is absent in solution as confirmed by NMR studies in different solvents. The presence of *meso*-furyl group alters the electronic properties of BODIPY which reflected in the down-field shifts in <sup>1</sup>H NMR, bathochromic shifts in absorption and emission bands compared to the *meso*-tolyl BODIPY. The electrochemical studies indicated that the *meso*-furyl BODIPYs are easier to reduce compared to *meso*-tolyl BODIPYs. DFT studies showed that the HOMO-LUMO energy gap is decreased in *meso*-furyl BODIPYs compared to *meso*-tolyl BODIPY which is in agreement with the experimental observations.

© 2011 Elsevier B.V. All rights reserved.

### 1. Introduction

Boron-dipyrromethene fluorophores (BODIPYs) have received much interest in various research fields as labeling reagents, fluorescent switches, chemosensors, light-harvesting systems and dye sensitized solar cells owing to their advantageous photophysical properties such as photostability, high absorption coefficients and high fluorescent quantum yields [1–3]. BODIPY dyes are amenable to modifications, and the properties can be fine-tuned by introduction of suitable substituents at appropriate positions of the boron-dipyrromethene framework. Various approaches have been attempted by different research groups to create new BODIPYs with altered electronic properties that include (1) introduction of electron-donating moieties [4–12], (2) replacement of *meso* C atom by a N atom [13–16], (3) rigidification of rotatable moieties [17–20], (4) extension of the  $\pi$ -conjugation [21–23], and (5) the extension of the  $\pi$ -conjugation by the fusion of aryl moieties [24,25]. Although all the above mentioned approaches have brought substantial changes in the electronic properties of the BODIPY dyes, there are relatively few reports on BODIPY dyes containing five membered heteroaryl moieties such as thienyl, furyl, pyrrole, imidazole etc in their framework [26,6,27,28]. Umezawa et al. [29] reported recently that the furan fused BODIPY dye **I** exhibited significant red-shifts in absorption and fluorescence spectral bands with very high fluorescence yields (Chart 1). Recently, it is reported that the substituents present at the 3,5-positions would be involved in intramolecular hydrogen bonding with

fluoride atoms which in turn would alter the electronic properties of boron-dipyrromethene [30]. Cohen and co-workers [30] showed that the two amide substituents at 3,5-positions in BODIPY **II** involved in intramolecular hydrogen bonding with boron-bound fluoride atoms help in rigidifying the chromophore resulting in significant alteration in electronic properties. Dehaen and co-workers [31,32] also showed the presence of intramolecular hydrogen bonding in their 3-anilino BODIPY **III** and 3,5-dianilino BODIPY **IV** compounds. These are few 3-monosubstituted or 3,5-disubstituted BODIPYs where the presence of intramolecular hydrogen-bonding alters the electronic properties of boron-dipyrromethenes. Interestingly, there is no report on BODIPY in which the *meso*-substituent is involved in intramolecular hydrogen-bonding with any atom on boron dipyrromethene core. In this paper, we report the examples of intramolecular hydrogen bonded *meso*-furyl dipyrromethenes **2–5** (Chart 2) in which the *meso*-furyl "O" is involved in hydrogen bonding with pyrrole "H" of boron-dipyrromethene core in solid state. While our study was in progress, Churchill and co-workers [33] reported the effect of five membered heteroaryl groups such as furyl, thienyl and selenyl at *meso*-position on structural and electronic properties of BODIPY. Interestingly, they did not discuss about the intramolecular hydrogen bonding present in **2** in solid state. Our study indicated that in *meso*-furyl BODIPYs **2**, **3** and **4**, the presence of intramolecular hydrogen bonding along with the small size of furyl group helps in reducing the dihedral angle between *meso*-furyl group and boron-dipyrromethene unlike *meso*-phenyl boron-dipyrromethene [35] in which the six membered phenyl group is relatively more out-of-plane orientation with the boron-dipyrromethene core. However, the hydrogen bonding is not present in solution for *meso*-furyl BODIPYs **2–5**

\* Corresponding author. Tel.: +91 22 5767176; fax: +91 22 5723480.

E-mail address: [ravikanth@chem.iitb.ac.in](mailto:ravikanth@chem.iitb.ac.in) (M. Ravikanth).

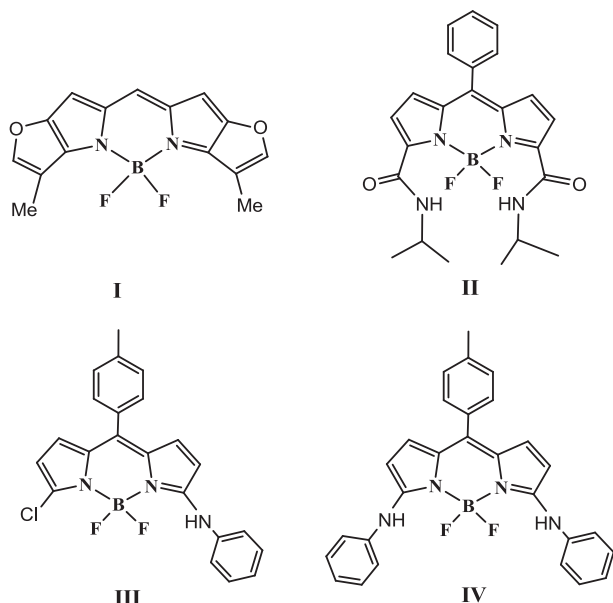


Chart 1. Molecular structures of BODIPYs I, II, III and IV.

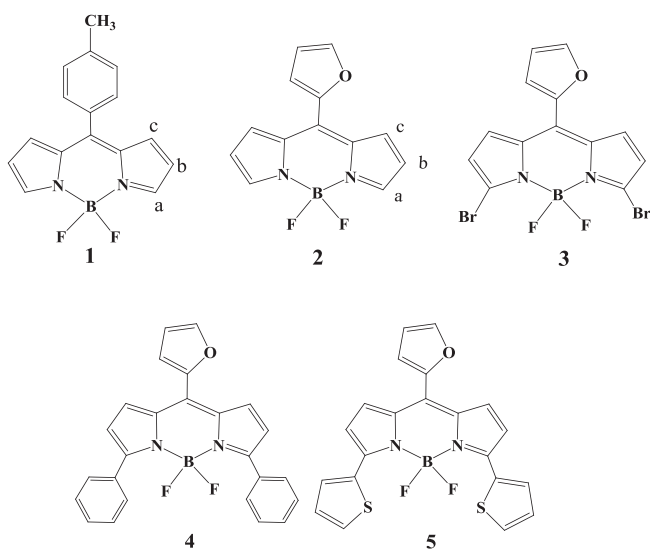


Chart 2. Molecular structures of Boron dipyrromethene dyes 1–5.

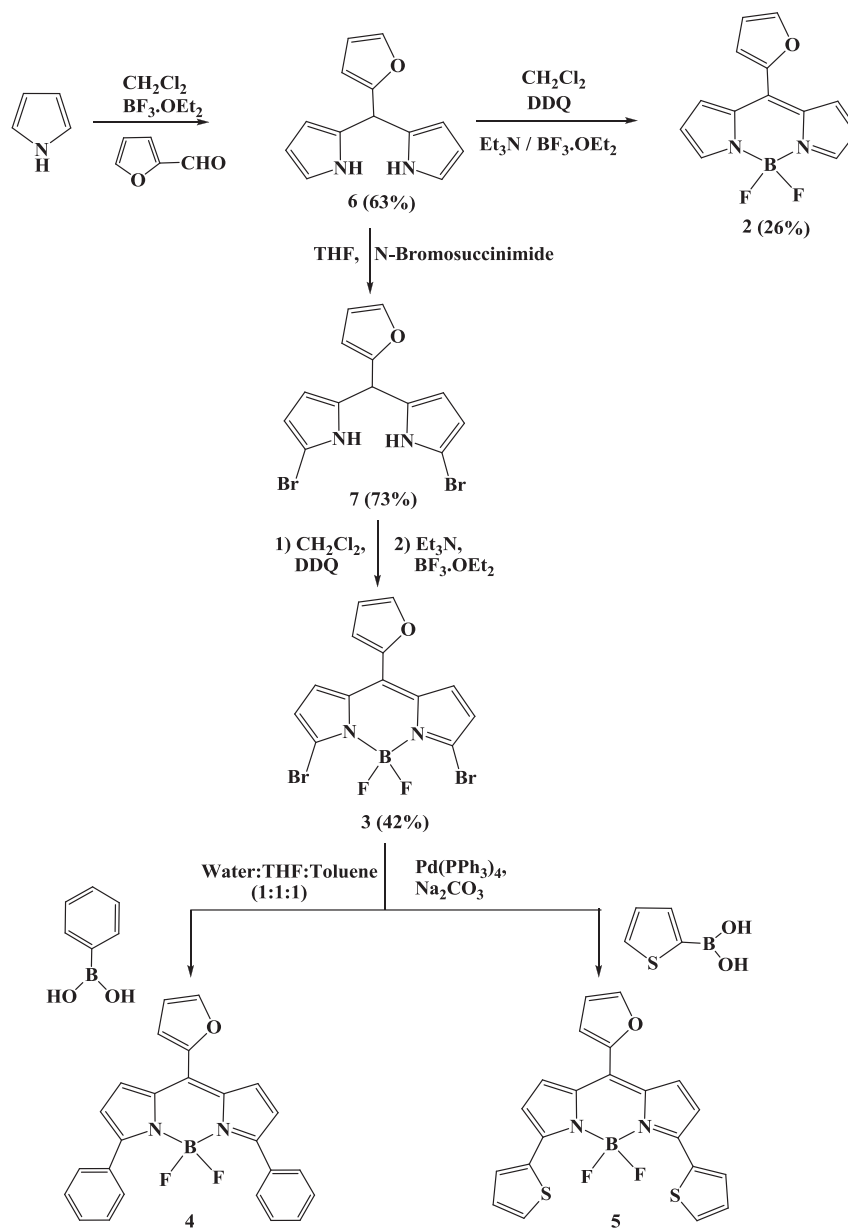
unlike Cohen's BODIPY **II** in which strong intramolecular hydrogen bonding is present in solution.

## 2. Results and discussion

The *meso*-tolyl boron-dipyrromethene **1** was prepared by following the literature procedure [36]. The *meso*-furyl boron-dipyrromethene **2** was prepared [33] as shown in Scheme 1. The required precursor, *meso*-furyl dipyrromethane **6** was prepared in 63% yield by treating one equivalent of furan-2-aldehyde with 25 equivalents of pyrrole in the presence of catalytic amount of  $\text{BF}_3 \cdot \text{OEt}_2$  at room temperature for 15 min [37]. In the next step, the compound **6** was first oxidized with DDQ in  $\text{CH}_2\text{Cl}_2$  at room temperature and then treated with triethylamine followed by  $\text{BF}_3 \cdot \text{OEt}_2$ . After standard work-up, the crude compound was purified by silica gel column chromatography and afforded **2** as dark red fluorescent solid in 26% yield. The 3,5-dibromo boron-dipyrro-

methene **3** was prepared in two steps (Scheme 1) by following our earlier reported method [37]. The compounds **4** and **5** were prepared in decent yields by treating compound **3** with phenyl-2-boronic acid and thienyl-2-boronic acid, respectively in the presence of  $\text{Pd}(\text{PPh}_3)_4$  in water/THF/toluene (1:1:1) at 80 °C. All reactions worked smoothly and compounds **2–5** are freely soluble in common organic solvents. The compounds **2–5** were confirmed by HR-MS mass spectral analysis and characterized by using various spectroscopic techniques. The compounds **2**, **3** and **4** were also characterized by X-ray crystallography.

The compounds **2–5** were characterized in detail by 1D, 2D,  $^{19}\text{F}$  and  $^{11}\text{B}$  NMR and the selected NMR data for compounds **2–5** along with compound **1** are presented in Table 1. The comparison of  $^1\text{H}$  NMR spectra of compounds **1** and **2** in selected region is shown in Fig. 1a and  $^1\text{H}$ - $^1\text{H}$  COSY NMR spectrum recorded for compound **2** is shown in Fig. 1b. The extensive NMR studies including  $^1\text{H}$ ,  $^{13}\text{C}$ ,  $^{19}\text{F}$  and  $^{11}\text{B}$  NMR for all compounds along with  $^1\text{H}$ - $^1\text{H}$  COSY, HSQC and HMBC NMR for compounds **2** and **4** helped in identifying the protons such as  $\beta$ -pyrrole protons represented as  $\text{H}_a$ ,  $\text{H}_b$  and  $\text{H}_c$  and *meso*-furyl protons represented as  $\text{H}_d$ ,  $\text{H}_e$  and  $\text{H}_f$  (Supporting information). The introduction of five membered furyl group at *meso*-position in place of six membered aryl group alter the electronic properties of boron-dipyrromethene core which clearly reflected in the downfield shift of certain protons [33]. In  $^1\text{H}$  NMR spectrum of **2**, the three pyrrole protons  $\text{H}_a$ ,  $\text{H}_b$  and  $\text{H}_c$  were observed as set of three signals at 7.89, 6.58 and 7.47 ppm, respectively and the three furyl protons  $\text{H}_d$ ,  $\text{H}_e$  and  $\text{H}_f$  were also observed as set of three signals at 7.83, 6.71 and 7.20 ppm, respectively. A close inspection of Fig. 1a and data in Table 1 indicates that the pyrrole protons  $\text{H}_a$  and  $\text{H}_b$  experienced slight shifts in **2** compared to **1**. However, the  $\text{H}_c$  proton of compound **2** experienced ca.  $\sim 0.5$  ppm downfield shift relative to compound **1**. Similarly, the corresponding carbons of  $\text{H}_a$ ,  $\text{H}_b$  and  $\text{H}_c$  in compound **2** also exhibited downfield shifts compared to **1** and maximum downfield shift was noted for carbon which possess  $\text{H}_c$  proton as judged by  $^{13}\text{C}$  NMR, HSQC and HMBC analysis. (Supporting information) Similar observations were made recently by Churchill and co-workers [33]. These results indicated that the  $\pi$ -delocalization is increased in **2** compared to **1** resulting in downfield shifts of pyrrole protons. This is because the *meso*-furyl group is smaller in compound **2** hence more in plane (as confirmed by X-ray crystallography) with the BODIPY core resulting in the extension of  $\pi$ -electron delocalization of BODIPY core into the *meso*-furyl group. On the other hand, the larger *meso*-tolyl group in compound **1** is more out-of-plane with the BODIPY core thus preventing the extension of  $p$ -delocalization into *meso*-tolyl group. The significant shift of  $\text{H}_c$  proton in **2** is because of its proximity to the furan "O" atom which provides more electron rich environment to  $\text{H}_c$  proton compared to  $\text{H}_a$  and  $\text{H}_b$  protons [33]. This is also clearly evident in 3,5-disubstituted *meso*-furyl boron-dipyrromethenes **3–5** which showed significant shifts for  $\text{H}_c$  proton compared to  $\text{H}_a$  and  $\text{H}_b$  protons (Table 1). However, the  $^{19}\text{F}$  and  $^{11}\text{B}$  NMR showed slight downfield shifts for compound **2** compared to compound **1** unlike Cohen's compound **II** which showed 16 ppm downfield shift in  $^{19}\text{F}$  NMR due to the presence of strong intramolecular hydrogen bonding between fluoride and amide group present at the 3,5-position of BODIPY. However, the  $^1\text{H}$  NMR spectra of compound **2** recorded in different solvents such as deuterated acetone, methanol and acetonitrile indicated that there is no intramolecular hydrogen bonding between *meso*-furyl "O" and the pyrrole  $\text{H}_c$  ( $\text{H}_3$  and  $\text{H}_7$ ) proton of boron dipyrin unit in solution (Supporting information). The  $^{19}\text{F}$  and  $^{11}\text{B}$  NMR of compounds **3**, **4** and **5** showed significant downfield shifts compared to **2** which is due to presence of substituents at 3,5-positions such as bromo, phenyl and thienyl groups, respectively.



**Scheme 1.** Synthesis of 3,5-disubstituted *meso*-furyl BODIPYs 2–5.

**Table 1**  
Comparison of  $^1\text{H}$ ,  $^{11}\text{B}$  and  $^{19}\text{F}$  NMR chemical shift values (in ppm) of compounds 1–5 recorded in  $\text{CDCl}_3$ .

Compound	$^1\text{H}$ NMR			$^{19}\text{F}$ NMR	$^{11}\text{B}$ NMR
	$\text{H}_a$	$\text{H}_b$	$\text{H}_c$		
<b>1</b>	7.94(s)	6.55(d)	6.89(d)	–145.27(q)	0.50(t)
<b>2</b>	7.89(s)	6.58(d)	7.47(d)	–145.94(q)	0.45(t)
<b>3</b>	–	6.68(d)	7.43(d)	–146.64(q)	0.75(t)
<b>4</b>	–	6.86(d)	7.48(d)	–132.99(q)	1.57(t)
<b>5</b>	–	6.58(d)	7.33(d)	–139.56(q)	1.86(t)

The orientation of *meso*-furyl group towards the plane of boron-dipyrromethene core is clearly evident in the crystal structures of compounds **2**, **3** and **4**. The single crystals of compounds **2**, **3** and **4** were obtained from *n*-hexane/dichloromethane on slow evaporation over a period of one week and crystallized in the monoclinic space groups  $P2_1/c$ ,  $P2_1/c$  and  $P2_1/n$ , respectively (Supporting

information). The X-ray structure of compound **2** and its packing diagram are shown in Fig. 2; the structures of **3** and **4** are shown in Fig. 3 and the relevant data of compounds **2**, **3**, **4** along with the reported *meso*-phenyl boron-dipyrromethene **8** [35] are presented in Table 2. The X-ray structures of **2**, **3** and **4** revealed that the dipyrin unit and the central six-membered ring containing the boron atom are almost coplanar with small deviations associated with either the attractive secondary interaction between furyl “O” or the repulsive interaction to minimize steric strain involving adjacent C-H’s on furyl ring and dipyrromethene. The plane defined by the F–B–F atoms is almost perpendicular to that of the boron-dipyrromethene core which is in line with the previously reported BODIPY **8** [35].

The most remarkable feature of X-ray crystal structures of compounds **2**, **3** and **4** compared to the reported compound **8** is the significant decrease in the dihedral angle ( $\text{C6–C5–C10–C11}$ ) between the *meso*-furyl group and the plane defining the various dipyrin atoms. In compound **8**, the *meso*-phenyl group is more out-of-plane

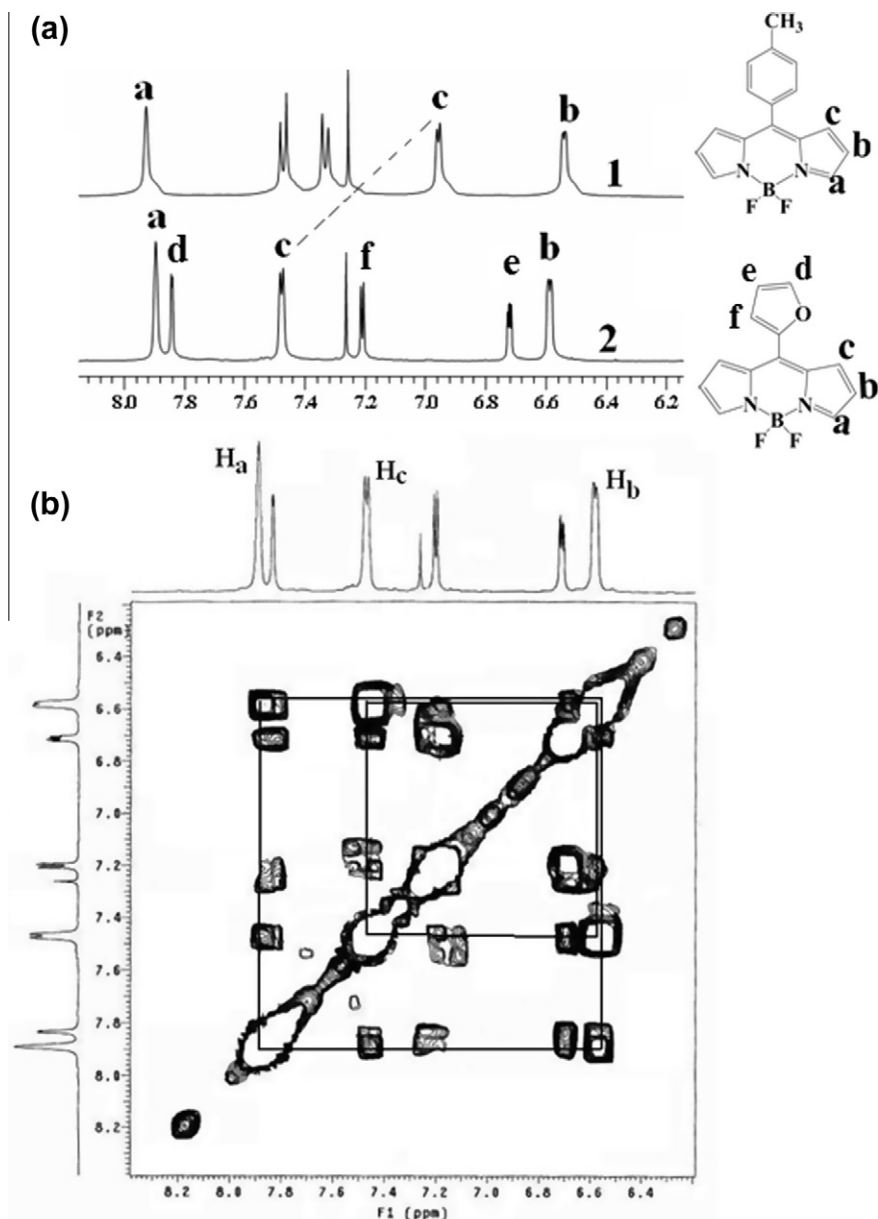


Fig. 1. (a) Comparison of <sup>1</sup>H NMR spectra of compounds **1** and **2** in selected region recorded in CDCl<sub>3</sub>. (b) <sup>1</sup>H-<sup>1</sup>H COSY spectrum for compound **2** recorded in CDCl<sub>3</sub>.

with dipyrin unit (dihedral angle of 52°) and the *meso*-phenyl group and dipyrin core are almost non-interactive [35]. However, in compounds **2**, **3** and **4**, the dihedral angle between *meso*-furyl group and the boron dipyrin frame-work are 25.1(3)°, 30.3(7)° and 31.0(3)°, respectively. Churchill and co-workers [33] also solved the crystal structure for compound **2** and observed the decrease in dihedral angle between *meso*-furyl group and the boron-dipyrin framework (~26.6°). These results indicate that the *meso*-furyl group is more in the plane of dipyrin unit resulting in strong interaction between the *meso*-furyl group and the boron dipyrin core in compounds **2–4**. The significant decrease in dihedral angle in compounds **2**, **3**, and **4** is attributed to the small size of furyl group and also to the presence of intramolecular hydrogen bonding between *meso*-furyl "O" and the pyrrole H<sub>c</sub> (H3 and H7) proton of dipyrin unit (O1...H3) as observed in their crystal structures. The *meso*-furyl "O" is engaged in hydrogen bonding with H<sub>c</sub> proton of the two pyrrole groups in dipyrin unit thus preventing the free rotation of *meso*-furyl group leading to the decrease of dihedral angle between *meso*-furyl group and dipyrin frame-work.

Furthermore, as evident in the packing diagram of **2** presented in Fig. 2b, one of the hydrogen atoms of the *meso*-furyl group is engaged in weak intermolecular hydrogen bonding with fluoride atom of another molecule forming a polymeric chain. In addition to hydrogen bonding, the two BODIPY molecules in asymmetric unit are arranged in such a way that there is a possibility of π-π stacking interaction between the pyrrole of one unit with the other and the distance between them is in the range of 3.4–3.8 Å [34]. Interestingly, Churchill and co-workers [33] did not discuss about intra and intermolecular hydrogen bonding and p-p stacking interactions noted here for *meso*-furyl boron dipyrromethenes. The bond-lengths such as B-F, B-N, C-N and bond angles such as N1-B1-N2, C4-C5-C6 in compounds **2**, **3** and **4** are also slightly altered compared to **1** which is attributed to the alteration of electronic properties due to the presence of furyl group at *meso*-position in compounds **2–4**.

The absorption, electrochemical and fluorescence properties of BODIPYs **2–5** were studied to understand the effect of *meso*-furyl group on the electronic properties of the boron-dipyrromethene

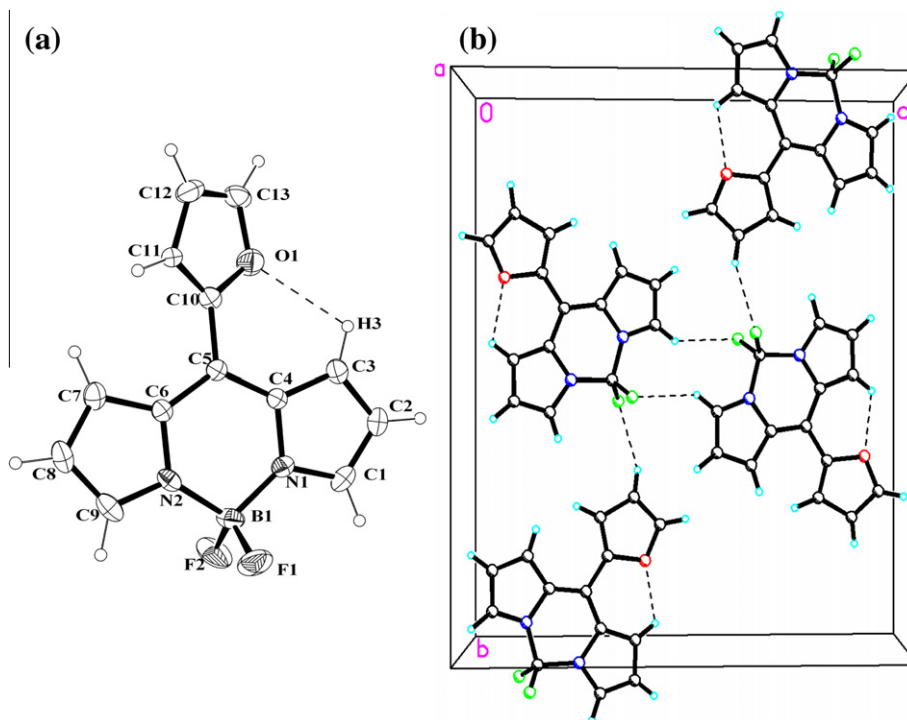


Fig. 2. Crystal structure of (a) compound **2** and (b) its packing diagram. Hydrogen bonds are denoted by dashed lines.

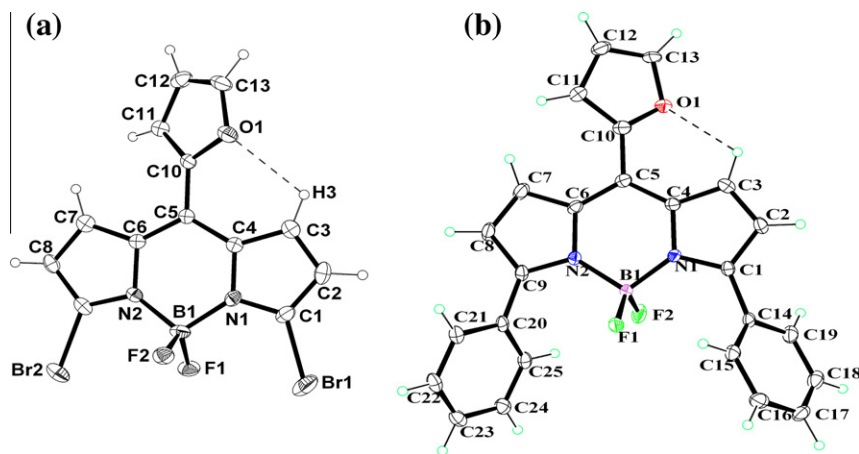


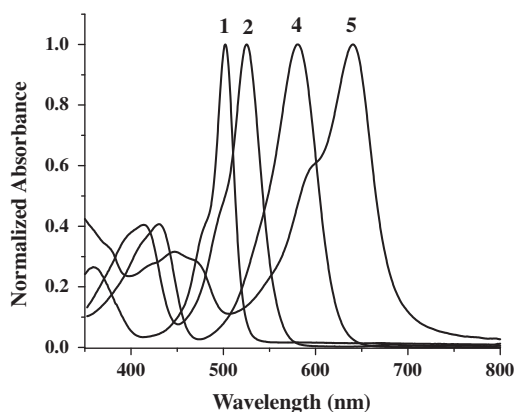
Fig. 3. Crystal structures of compounds (a) **3** and (b) **4** with hydrogen bonds denoted by dashed lines.

core. The absorption properties of compounds **1**, **2**, **4** and **5** were studied in six different solvents of varying polarity. The comparison of normalized absorption spectra of compounds **1**, **2**, **4** and **5** recorded in toluene is shown in Fig. 4 and the data for compounds **1**, **2**, **4** and **5** recorded in six different solvents are presented in Table 3. Generally, the *meso*-aryl substituted BODIPYs such as **1** show two absorption bands [35]: (1) a strong  $S_0 \rightarrow S_1$  transition with a maximum appearing at 502 nm and (2) the second maximum or shoulder on the high energy side, centered at about 480 nm, which is attributed to the  $0 \rightarrow 1$  vibrational transition. In addition, a considerably weaker, broad absorption band at 375 nm corresponding to  $S_0 \rightarrow S_2$  transition is also present. The absorption properties of *meso*-furyl boron-dipyrromethene **2** showed some similarities and differences compared to **1**. The absorption spectrum of **2** is similar in shape as that of **1**. It exhibits a strong absorption band at 525 nm with a shoulder at 485 nm and relatively more intense band at 402 nm. However, as compared to compound **1**, the absorption

spectrum of **2** exhibited  $873 \text{ cm}^{-1}$  bathochromic shift in  $S_0 \rightarrow S_1$  transition. Furthermore, the absorption band of **2** is very broad with full-width at half maximum (FWHM) of  $1819 \text{ cm}^{-1}$  compared to **1** which show relatively narrow band with FWHM of  $1166 \text{ cm}^{-1}$  in toluene. The absorption spectrum of **2** is not affected much by solvent polarity and the maximum being slightly shifted hypsochromically when the solvent is changed from toluene (525 nm) to acetonitrile (516 nm) which is consistent with the general behavior of BODIPY chromophores [38–45]. This small shift reflects the polarizability of the solvent. In all solvents, the compound **2** experienced similar bathochromic shift of  $S_0 \rightarrow S_1$  band with change in FWHM compared to **1**. The  $S_0 \rightarrow S_2$  band did not show any variation in peak maxima and band width on changing the polarity of the solvent. Upon introduction of aryl substituents at 3,5-positions such as phenyls in **4** and thienyls in **5** resulted in further bathochromic shift in  $S_0 \rightarrow S_1$  transition with more FWHM and the maximum effect was observed for compound **5**. This is

**Table 2**  
Selected Bond Distances (Å) and Bond Angles (°) for compounds **2**, **3** and **4** along with **8**.

Bond length/torsion angles	<b>8</b>	<b>2</b>	<b>3</b>	<b>4</b>
B1–F1	1.381(10)	1.385(3)	1.380(6)	1.3763(19)
B1–N1	1.547(9)	1.531(3)	1.551(7)	1.544(2)
N1–C1	1.345(8)	1.345(3)	1.331(6)	1.3594(16)
N1–C4	1.389(8)	1.393(3)	1.382(6)	1.3975(16)
O1...Hc <sup>a</sup>	–	2.38	2.38	2.48
C3–H3	0.95	0.95	0.95	0.95
C2–C3	1.387(10)	1.374(3)	1.367(7)	1.369(2)
C5–C10	1.47	1.451(3)	1.439(6)	1.4544(19)
O(1)–C(10)	–	1.364(2)	1.374(6)	1.282(2)
O(1)–C(13)	–	1.382(3)	1.370(6)	1.362(5)
F1–B1–F2	110.29(12)	110.0(2)	110.0(4)	110.76(12)
O1–H3...C3	–	110.21	110.95	108.93
N1–B1–N2	106.39(8)	106.16(18)	106.3(4)	106.84(11)
C(4)–C(5)–C(6)	120.17(4)	120.45(17)	120.1(4)	120.58(12)
C(10)–O(1)–C(13)	–	105.41(18)	106.2(4)	107.5(3)
C(4)–C(5)–C(10)–O(1)	–	25.0(3)	26.4(6)	35.4(3)
C(6)–C(5)–C(10)–C(11)	52.5(3)	25.1(3)	30.3(7)	31.0(3)
C(10)–C(5)–C(6)–C(7)	6.2(4)	2.4(3)	3.3(7)	8.8(3)
C(3)–C(4)–C(5)–C(10)	3.5(4)	1.4(3)	7.6(7)	2.7(2)

<sup>a</sup> H<sub>c</sub> is H<sub>3</sub>/H<sub>7</sub>.**Fig. 4.** Comparison of normalized absorption spectra of compounds **1**, **2**, **4** and **5** recorded in toluene.**Table 3**  
Photophysical data of BODIPY compounds **1**, **2**, **4** and **5** in different solvents. Concentration used was  $5 \times 10^{-6}$  M.

Compound	Solvent	$\lambda_{\text{abs}}$ (nm)	$\epsilon$	FWHM ( $\text{cm}^{-1}$ )	$\lambda_{\text{em}}$ (nm)	$\Delta\nu_{\text{st}}$ ( $\text{cm}^{-1}$ )	$\Phi$
<b>1</b>	Toluene	502	4.68	1166	520	690	0.053
	CHCl <sub>3</sub>	501	4.73	1085	517	618	0.042
	THF	502	4.68	1379	521	626	0.023
	Ethyl acetate	497	4.74	1200	514	665	0.017
	MeOH	496	4.76	1226	513	668	0.017
	MeCN	495	4.75	1240	513	709	0.010
<b>2</b>	Toluene	525	4.40	1819	573	1596	0.058
	CHCl <sub>3</sub>	523	4.50	1703	568	1515	0.057
	THF	520	4.48	1628	569	1656	0.036
	Ethyl acetate	518	4.49	2015	563	1543	0.050
	MeOH	516	4.49	2058	562	1587	0.032
	MeCN	516	4.50	1352	564	1650	0.027
<b>4</b>	Toluene	580	4.72	2154	648	1810	0.025
	CHCl <sub>3</sub>	577	4.72	2335	647	1876	0.021
	THF	576	4.73	2464	645	1858	0.033
	Ethyl acetate	576	4.77	2177	635	1887	0.021
	MeOH	569	4.61	2223	626	1600	0.016
	MeCN	566	4.68	2223	624	1642	0.020
<b>5</b>	Toluene	647	4.61	1985	684	836	0.012
	CHCl <sub>3</sub>	645	4.55	2303	680	798	0.016
	THF	641	4.64	1975	675	786	0.042
	Ethyl acetate	636	4.61	1993	674	887	0.037
	MeOH	634	4.62	2235	673	914	0.055
	MeCN	632	4.48	2428	672	942	0.041

probably due to further enhancement of conjugation in BODIPY unit because of the presence of aryl substituents at 3,5-positions. Compounds **4** and **5** also exhibited similar hypsochromic shifts on changing the polarity of the solvent.

The electrochemical properties of BODIPYs **1**, **2**, **4** and **5** were investigated by cyclic voltammetry at a scan rate of 50 mV/s using tetrabutylammonium perchlorate as supporting electrolyte. A comparison of reduction waves of compounds **1**, **2**, **4** and **5** is shown in Fig. 5 and redox potential data are presented in Table 4. The BODIPYs generally show one irreversible oxidation, one reversible reduction and one quasi-reversible reduction. As clearly revealed from Fig. 5 and data in Table 4 that the first reduction potential of the *meso*-furyl boron dipyrromethene **2** is shifted towards less negative compared to *meso*-tolyl boron dipyrromethene **1** by  $\sim 165$  mV. This suggests that the compound **2** is much easier to reduce as compared to compound **1**. However, the compound **4** containing two phenyl groups at 3,5-positions is difficult to reduce than compound **2** whereas the compound **5** containing two

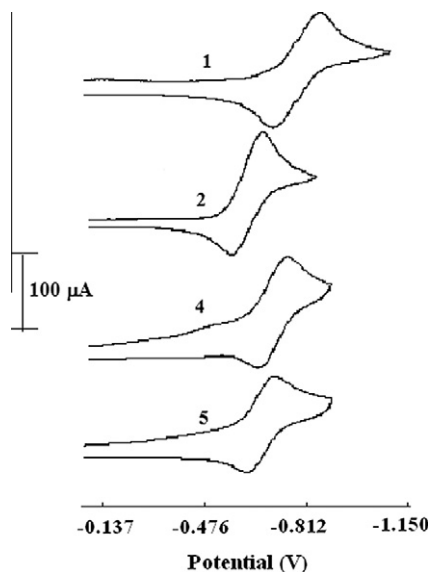


**Fig. 5.** Comparison of reduction wave of cyclic voltammograms of compounds **1**, **2**, **4** and **5** recorded in  $\text{CH}_2\text{Cl}_2$  containing 0.1 M TBAP as the supporting electrolyte recorded at a scan speed of 50 mV/s.

thienyl groups at 3,5-positions is equally easier to reduce like compound **2**. Thus, the electrochemical study clearly indicated that *meso*-furyl BODIPYs **2–5** were easier to reduce compared to the *meso*-tolyl BODIPY **1**.

**Table 4**

Electrochemical redox data (V) of compounds **1**, **2**, **4** and **5** in dichloromethane containing 0.1 M TBAP as supporting electrolyte.

Compound	Oxidation	Reduction	
		I	II
<b>1</b>	–	–0.788	–1.81
<b>2</b>	1.41	–0.622	–1.74
<b>4</b>	1.36	–0.736	–1.63
<b>5</b>	1.14	–0.628	–1.56

The fluorescence properties of **1**, **2**, **4** and **5** are also studied in six solvents (Table 3). The comparison of normalized fluorescence spectra of compounds **1**, **2**, **4** and **5** recorded in toluene is shown in Fig. 6a. The compounds **2**, **4** and **5** exhibited significant differences in fluorescence properties compared to **1** which are outlined as follows: (1) the emission band of compound **2** exhibited  $1778\text{ cm}^{-1}$  red shift compared to **1**. However, among *meso*-furyl boron-dipyrromethenes **2**, **4** and **5**, the compound **5** showed maximum red shift in emission maxima; (2) the fluorescence band of **2**, **4** and **5** is very broad compared to **1** (Fig. 6a); (3) compound **2** exhibited large Stokes shift compared to **1** (Fig. 6b and c). Among compounds **2**, **4** and **5**, compound **5** showed less Stokes shift and **4** showed maximum Stokes shift; (4) the quantum yield of **2** and **1** is almost same whereas the compounds **4** and **5** showed lower quantum yield compared to **2**. The observations were similar in all six solvents. The lower quantum yield of compound **4** requires detailed investigation. The large red-shifts observed for *meso*-furyl BODIPYs **2**, **4** and **5** are attributed to the enhancement of  $\pi$ -electron conjugation due to increased co-planarity of *meso*-furyl group with

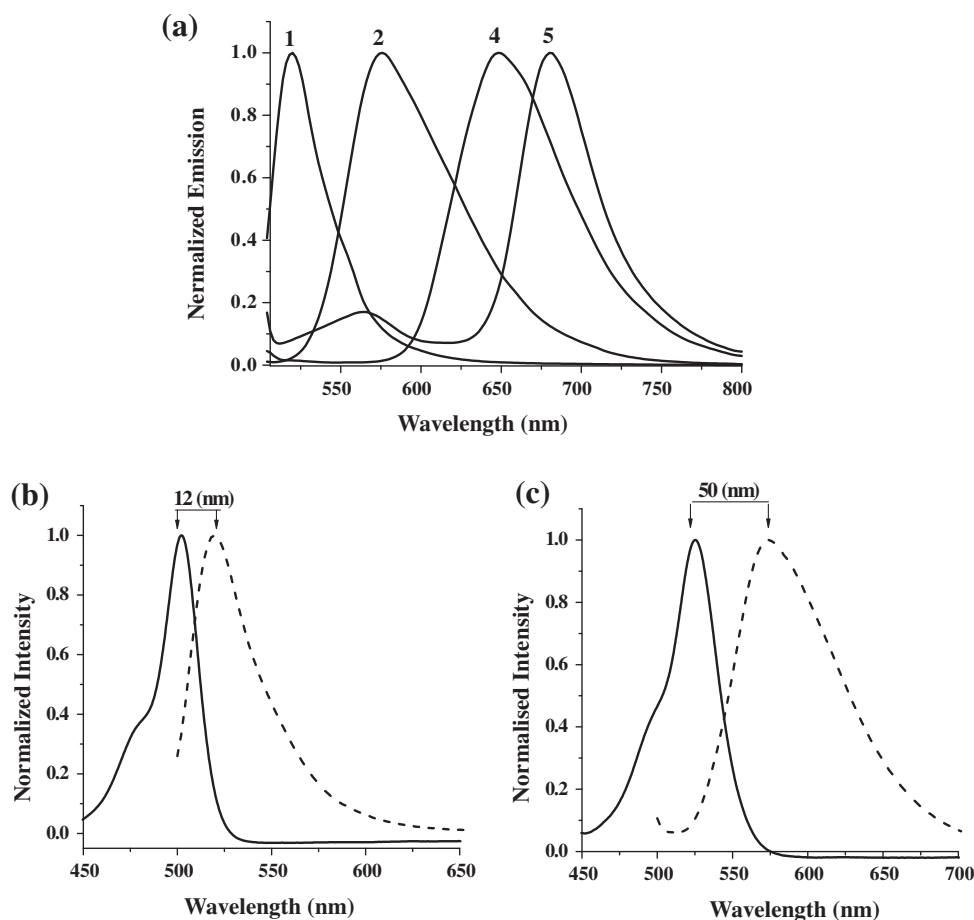


**Fig. 6.** (a) Comparison of normalized emission spectra of compounds **1**, **2**, **4** and **5** recorded in toluene using  $\lambda_{\text{ex}} = 488\text{ nm}$ . (b) Comparison of absorption (—) and emission (---) spectra of **1** in toluene. (c) Comparison of absorption (—) and emission (---) spectra of **2** in toluene.

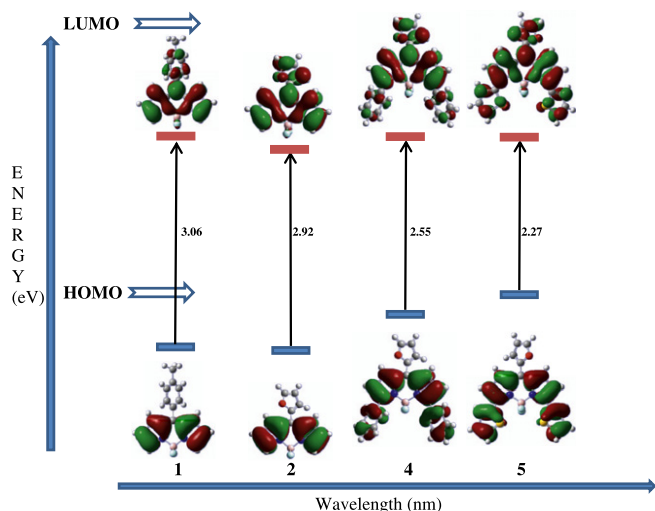


Fig. 7. Orbital-correlation diagram of HOMO and LUMO (FMO's) for compounds **1**, **2**, **4** and **5**.

boron-dipyrromethene unit and also partly because of the presence of substituents at 3,5-positions. The large Stokes shifts noted for **2** and **4** in different solvents support the enhancement of Franck-Condon factor due to substantial structural reorganization in the excited state.

In order to understand the differences between the electronic properties of compounds **1**, **2**, **4** and **5**, quantum chemical calculations were performed using DFT method. A qualitative analysis of the electronic distribution in HOMO and LUMO states (Fig. 7) on these molecules suggested that there were very minute differences between compounds **1** and **2**. These compounds were found to be very similar in electronic distribution in HOMO and LUMO states particularly in the main BODIPY nucleus. A close examination of the LUMO states of compounds **1** and **2** revealed that electrons were more delocalized in 2-furyl ring as compared to *p*-tolyl group. Such a comparison clearly revealed that the 2-furyl group is involved in FMOs (HOMOs and LUMOs) to a greater extent to bring down the gap in the energies through some electronic interaction. For compounds **4** and **5**, the significant changes were observed in the HOMO and LUMO electronic distribution. For these compounds, the electronic distribution in the HOMO and LUMO states was delocalized away from the BODIPY nucleus. Such an effect can be attributed to be arisen through extension of  $\pi$ -conjugation. The quantitative differences were found among the compounds **1** and **2** for their HOMO, LUMO energies and their gaps. It is interesting to note that the values for HOMO–LUMO gap of compound **2** is less than **1** indicating the existence of some stabilizing force. Compounds **4** and **5** were found to have least energy gaps between the FMOs. As shown in Fig. 7, the gaps in the energies of HOMOs and LUMOs follow the order as  $1 > 2 > 4 > 5$ . The decrease in the HOMO–LUMO energy gap is in agreement with the observed red shifts of absorption and emission bands. The decrease in the reduction potential of compounds **2**, **4** and **5** compared to **1** is clearly reflected through the stabilization of LUMO states of these compounds. Precisely speaking, for compounds **4** and **5**, this effect was solely observed due to elevation of HOMO energies (Table S2 in Supporting information). Thus the quantum mechanics based studies of HOMO and LUMO states of these molecules were found to be in agreement with the experimental results.

### 3. Conclusions

We described the synthesis of four *meso*-furyl boron-dipyrromethene dyes and their absorption, electrochemical and fluores-

cence properties. It was found through, both the experimental facts and computational approach that on replacement of six membered *meso*-aryl group with five membered furyl group alter the electronic properties of the boron-dipyrromethene dye significantly. The introduction of *meso*-furyl group in place of *meso*-phenyl group lead to down field shifts in the chemical shifts of pyrrole protons, bathochromic shifts in absorption and emission bands with increase in full width at half maximum, relatively large Stoke's shifts and easier reductions. These changes in *meso*-furyl BODIPYs were attributed to in-plane orientation of *meso*-furyl group with the plane of the boron-dipyrromethene and assisting the enhancement of  $\pi$ -conjugation unlike *meso*-tolyl boron-dipyrromethene in which the six membered tolyl group is not in plane with the boron-dipyrromethene and preventing the  $\pi$ -conjugation as confirmed by their X-ray crystal structures.

## 4. Experimental

### 4.1. General

The known compounds **2**, **3**, **6** and **7** were prepared by following the reported procedures [33,37]. THF and toluene were dried over sodium benzophenone ketyl and chloroform, ethyl-acetate, methanol, acetonitrile were dried over calcium hydride and distilled prior to use.  $\text{BF}_3 \cdot \text{OEt}_2$  and 2,3-dichloro-5,6-dicyano-1,4-benzoquinone (DDQ) obtained from Spectrochem (India) were used as obtained. All other chemicals used for the synthesis were reagent grade unless otherwise specified. Column chromatography was performed on silica (60–120 mesh).

### 4.2. Instrumentation

$^1\text{H}$  NMR spectra ( $\delta$  in ppm) were recorded using Varian VXR 300 and 400 MHz and Bruker 400 MHz NMR spectrometer.  $^{13}\text{C}$  NMR spectra were recorded on Varian and Bruker spectrometer operating at 100.6 MHz.  $^{19}\text{F}$  NMR spectra were recorded on Varian spectrometer operating at 282.2 MHz.  $^{11}\text{B}$  NMR spectra were recorded on Varian spectrometer operating at 96.3 MHz. TMS was used as an internal reference for recording  $^1\text{H}$  (of residual proton;  $\delta$  7.26) and  $^{13}\text{C}$  ( $\delta$  77.0 signal) in  $\text{CDCl}_3$ . Absorption and steady-state fluorescence spectra were obtained with Perkin–Elmer Lambda-35 and PC1 Photon Counting Spectrofluorometer manufactured by ISS, USA instruments, respectively. Fluorescence spectra were recorded at 25 °C in a 1 cm quartz fluorescence cuvette. The fluorescence quantum yields ( $\Phi_f$ ) were estimated from the emission and absorption spectra by comparative method at the excitation wavelength of 488 nm using Rhodamine 6G ( $\Phi_f = 0.88$ ) [31] as standard. Cyclic voltammetric (CV) and differential pulse voltammetric (DPV) studies were carried out with electrochemical system utilizing the three electrode configuration consisting of a glassy carbon (working electrode), platinum wire (auxiliary electrode) and saturated calomel (reference electrode) electrodes. The experiments were done in dry dichloromethane using 0.1 M tetrabutylammonium perchlorate as supporting electrolyte. Half wave potentials were measured using DPV and also calculated manually by taking the average of the cathodic and anodic peak potentials. MALDI-TOF spectra were obtained from Axima-CFR manufactured by Kratos Analyticals.

### 4.3. X-ray diffraction studies

The single crystals of compounds **2** (CCDC-768790), **3** (CCDC-768788) and **4** (CCDC-768789) were obtained on slow evaporation of *n*-hexane/dichloromethane over a period of one week. The intensity data collection for compounds **2**, **3** and **4** have been

carried out on a Nonius MACH3 four circle diffractometer at 293 K. Structure solutions for the compounds **2**, **3** and **4** were obtained using direct methods (SHELXS-97) [46] and refined using full-matrix least-squares methods on  $F^2$  using SHELXL-97 [47]. Compounds **2** and **3** were crystallized with two molecules in the asymmetric unit. There are no statistically significant differences in the metrical parameters for the two molecules. In each molecule, the furyl ring is disordered over two conformations.

#### 4.4. Computational studies

The computational studies were performed with GAUSSIAN 03 [48] installed on a windows operating system. The structures were extracted from the X-ray diffraction output files generated. Initial structural rectifications, atom and bond typing and addition of hydrogen atoms were done with Chem3D utility in Chemoffice. For these studies, some conformers representing two possible rotations of meso-furyl ring around BODIPY nucleus were also generated from the structures as templates. The structures were energy optimized using quantum mechanics with density functional theory (DFT) and B3LYP gradient corrected correlation functional method in conjugation with standard 6-31G (p,d) basis set and parameters. For the optimized structures, we carried out complete full population analyses.

#### 4.5. 3,5-Diphenyl-8-(2-furyl)-4,4-difluoro-4-bora-3a,4a-diaza-s-indacene (**4**)

Two neck 100 mL round bottom flask fixed with a reflux condenser was degassed with  $N_2$  for few minutes. Samples of **3** (100 mg, 0.60 mmol), phenyl-boronic acid (387 mg, 3.04 mmol) and  $Na_2CO_3$  (256 mg, 2.44 mmol) in water/THF/toluene (1:1:1) 15 ml was stirred under  $N_2$  for 5 min.  $Pd(PPh_3)_4$  (68 mg, ~5–10 mol%), was added and the reaction mixture was refluxed at 80 °C. After completion of the reaction as judged by TLC analysis, the reaction mixture was diluted with water (5 ml) and extracted with diethyl ether. The combined organic layers were washed with water, brine and dried over  $MgSO_4$ . The solvent was evaporated and the crude product was purified on a silica gel column using petroleum ether/ethyl acetate 95:5 to afford 3,5-diphenyl-8-(phenyl)-4,4-difluoro-4-bora-3a,4a-diaza-s-indacene **4** in 75% yield.  $^1H$  NMR (400 MHz,  $CDCl_3$ ,  $\delta$  in ppm): 6.68 (d,  $J = 4.27$  Hz, 2H, pyrrole), 6.73 (s, 1H, furan), 7.09 (d,  $J = 3.36$  Hz, 1H, furan), 7.40–7.44 (m, 8H, phenyl), 7.83 (s, 1H, furan), 7.86 (d,  $J = 6.72$  Hz, 4H, pyrrole + phenyl).  $^{13}C$  NMR (100 MHz,  $CDCl_3$ ,  $\delta$  in ppm): 113.0, 118.8, 121.0, 128.3, 129.5, 130.3, 132.9, 134.0, 146.7, 149.0, 158.5, 168.2.  $^{19}F$  NMR (282.2 MHz,  $CDCl_3$ ,  $\delta$  in ppm): –132.99 (q,  $J_{B-F} = 64.0$  Hz).  $^{11}B$  NMR (96.3 MHz,  $CDCl_3$ ,  $\delta$  in ppm): 1.57 (t,  $J_{B-F} = 32.0$  Hz). MALDI-TOF:  $m/z = 408.5$   $[M-1]^+$ . HRMS calcd for ( $C_{25}H_{17}BF_2N_2O$ ): 391.1418  $[M-19]^+$  found 391.1399  $[M-19]^+$ .

#### 4.6. 3,5-Di(2-thienyl)-8-(2-furyl)-4,4-difluoro-4-bora-3a,4a-diaza-s-indacene (**5**)

Compound **5** was prepared by following the same procedure as for compound **4** using thiophene-2-boronic acid. The crude compound was purified on silica column using petroleum ether as an eluent and obtained the pure compound **5** in 33% yield.  $^1H$  NMR (400 MHz,  $CDCl_3$ ,  $\delta$  in ppm): 6.67 (s, 1H, furan), 6.86 (d,  $J = 4.58$  Hz, 2H, pyrrole), 6.98 (d,  $J = 2.74$  Hz, 1H, furan), 7.18 (m, 2H, thiophene), 7.32 (d,  $J = 3.97$  Hz, 2H, thiophene), 7.48 (d,  $J = 4.27$  Hz, 2H, pyrrole), 7.76 (s, 1H, furan), 8.18 (d,  $J = 3.05$  Hz, 2H, thiophene).  $^{19}F$  NMR (282.2 MHz,  $CDCl_3$ ,  $\delta$  in ppm): –139.68 (q,  $J_{B-F} = 64.0$  Hz).  $^{11}B$  NMR (96.3 MHz,  $CDCl_3$ ,  $\delta$  in ppm): 1.86 (t,  $J_{B-F} = 32.07$  Hz). MALDI-TOF:  $m/z = 420.6$   $[M-1]^+$ . HRMS calcd for ( $C_{21}H_{13}BF_2N_2OS_2$ ): 403.0546  $[M-19]^+$  found: 403.0548  $[M-19]^+$ .

## Acknowledgment

M.R. thanks CSIR and DST for financial support. T.K.K. thanks Indian Institute of Technology for fellowship. We thank the DST funded National Single Crystal X-ray Diffraction Facility for diffraction data. We also thank Dr. Evans Coutinho (Bombay College of Pharmacy) for providing computational facility.

## Appendix A. Supplementary material

$^1H$ ,  $^1H-^1H$  COSY, HSQC, HMBC,  $^{13}C$ ,  $^{19}F$  and  $^{11}B$  NMR spectra and mass spectra of all compounds. Supplementary data associated with this article can be found, in the online version, at doi:10.1016/j.ica.2011.11.017.

## References

- [1] R. Ziessel, G. Ulrich, A. Harriman, *New J. Chem.* 31 (2007) 496.
- [2] A. Loudet, K. Burgess, *Chem. Rev.* 107 (2007) 4891.
- [3] G. Ulrich, R. Ziessel, A. Harriman, *Angew. Chem., Int. Ed.* 47 (2008) 1184.
- [4] M. Kollmannsberger, T. Gareis, S. Heinel, J. Daub, J. Breu, *Angew. Chem., Int. Ed.* 36 (1997) 1333.
- [5] K. Rurack, M. Kollmannsberger, U. Resch-Genger, J. Daub, *J. Am. Chem. Soc.* 122 (2000) 968.
- [6] T. Matsumoto, Y. Urano, T. Shoda, H. Kojima, T. Nagano, *Org. Lett.* 9 (2007) 3375.
- [7] S. Zrig, P. Remy, B. Andrioletti, E. Rose, I. Asselberghs, K. Clays, *J. Org. Chem.* 73 (2008) 1563.
- [8] A.C. Benniston, G. Copley, A. Harriman, D.B. Rewinska, R.W. Harrington, W. Clegg, *J. Am. Chem. Soc.* 130 (2008) 7174.
- [9] E. Lager, J. Liu, A. Aguilar-Aguilar, B.Z. Tang, E. Peña-Cabrera, *J. Org. Chem.* 74 (2009) 2053.
- [10] X. Yin, L. Yongjun, L. Yuliang, Y. Zhu, X. Tang, H. Zheng, D. Zhu, *Tetrahedron* 65 (2009) 8373.
- [11] R. Ziessel, P. Retailleau, K.J. Elliott, A. Harriman, *Chem. Eur. J.* 15 (2009) 10369.
- [12] M.R. Rao, K.V.P. Kumar, M. Ravikanth, *J. Organomet. Chem.* 695 (2010) 863.
- [13] A. Coskun, M.D. Yilmaz, E.U. Akkaya, *Org. Lett.* 9 (2007) 607.
- [14] A. Loudet, R. Bandichhor, K. Burgess, A. Palma, S.O. McDonnell, M.J. Hall, D.F. O'Shea, *Org. Lett.* 10 (2008) 4771.
- [15] A. Palma, M. Tasiar, D.O. Frimannsson, T. Vu, R. Méallet-Renault, D.F. O'Shea, *Org. Lett.* 11 (2009) 3638.
- [16] J. Murtagh, D.O. Frimannsson, D.F. O'Shea, *Org. Lett.* 11 (2009) 5386.
- [17] B.A. Trofimov, *Adv. Heterocycl. Chem.* 51 (1990) 177.
- [18] A.B. Zaitsev, R. Meallet-Renault, E.Y. Schmidt, A.I. Mikhaleva, S. Barde, C. Dumas, A.M. Vasil'tsov, N.V. Zorina, R.B. Pansu, *Tetrahedron* 61 (2005) 2683.
- [19] K. Rurack, U. Resch-Genger, *Chem. Soc. Rev.* 31 (2002) 116.
- [20] Y. Mei, P.A. Bentley, W. Wang, *Tetrahedron Lett.* 47 (2009) 2447.
- [21] A. Burghart, H. Kim, M.B. Welch, T. Joe Reibenspies, K. Burgess, *J. Org. Chem.* 64 (1999) 7813.
- [22] L. Bonardi, G. Ulrich, R. Ziessel, *Org. Lett.* 10 (2008) 2183.
- [23] M. Bröring, R. Krüger, S. Link, C. Kleeberg, S. Köhler, X. Xie, B. Ventura, L. Flamigni, *Chem. Eur. J.* 14 (2008) 2976.
- [24] T. Kowada, S. Yamaguchi, K. Ohe, *Org. Lett.* 12 (2010) 296.
- [25] A. Nagai, Y. Chujo, *Macromolecules* 43 (2010) 193.
- [26] S.H. Choi, K. Kim, J. Lee, Y. Do, D.G. Churchill, *J. Chem. Crystallogr.* 37 (2007) 315.
- [27] E. Peña-Cabrera, A. Aguilar-Aguilar, M.G. Domínguez, E. Lager, R.Z. Vázquez, J.G. Vargas, F.V. Garcia, *Org. Lett.* 9 (2007) 3985.
- [28] S.H. Choi, K. Kim, J. Jeon, B. Meka, D. Buccella, K. Pang, S. Khatua, J. Lee, D.G. Churchill, *Inorg. Chem.* 47 (2008) 11071.
- [29] K. Umezawa, Y. Nakamura, H. Makino, D. Citterio, K. Suzuki, *J. Am. Chem. Soc.* 130 (2008) 1550.
- [30] J.A. Jacobsen, J.R. Stork, D. Magde, S.M. Cohen, *Dalton Trans.* 39 (2010) 957.
- [31] W. Qin, V. Leen, T. Rohand, W. Dehaen, P. Dedecker, M. Van, K. der Auweraer, L. Robeyns, D. Van Meervelt, B. Beljonne, J.N. Van Aeverbeke, K. Clifford, K. Driesen, N. Binnemans, N. Boens, *J. Phys. Chem. A* 113 (2009) 439.
- [32] W. Qin, V. Leen, W. Dehaen, J. Cui, C. Xu, X. Tang, W. Liu, T. Rohand, D. Beljonne, B. Van Aeverbeke, J.N. Clifford, K. Driesen, K. Binnemans, M. Van der Auweraer, N. Boens, *J. Phys. Chem. C* 113 (2009) 11731.
- [33] K. Kim, C. Jo, S. Easwaramoorthi, J. Sung, D.H. Kim, D.G. Churchill, *Inorg. Chem.* 49 (2010) 4881.
- [34] A. Nagai, J. Miyake, K. Kokado, Y. Nagata, Y. Chujo, *J. Am. Chem. Soc.* 130 (2008) 15276.
- [35] H.L. Kee, C. Kirmaier, L. Yu, P. Thamyongkit, W.J. Youngblood, M.E. Calder, L. Ramos, B.C. Noll, D.F. Bocian, W.R. Scheidt, R.R. Birge, J.S. Lindsey, D. Holten, *J. Phys. Chem. B* 109 (2005) 20433.
- [36] R.W. Wagner, J.S. Lindsey, *Pure Appl. Chem.* 68 (1996) 1373.
- [37] T.K. Khan, M.R. Rao, M. Ravikanth, *Eur. J. Org. Chem.* (2010) 2314–2323.
- [38] M. Kollmannsberger, K. Rurack, U. Resch-Genger, J. Daub, *J. Phys. Chem. A* 102 (1998) 10211.
- [39] F. Amat-Guerri, *Chem. Phys. Lett.* 299 (1999) 315.

- [40] K. Rurack, M. Kollmannsberger, J. Daub, *Angew. Chem., Int. Ed.* 40 (2001) 385.
- [41] R.Y. Lai, A.J. Bard, *J. Phys. Chem. B* 107 (2003) 5036.
- [42] F. López Arbeloa, J. Bañuelos Prieto, V.M. Martínez, T. Arbeloa López, I. López, *Chem Phys Chem* 5 (2004) 1762.
- [43] B. Ventura, G. Marconi, M. Bröring, R. Krüger, L. Flamigni, *New J. Chem.* 33 (2009) 428.
- [44] K. Guzow, K. Kornowska, W. Wicz, *Tetrahedron Lett.* 50 (2009) 2908.
- [45] K. Cieřlik-Boczula, K. Burgess, L. Li, B. Nguyen, L. Pandey, W.M. De Borggraeve, M. Van der Auweraer, N. Boens, *J. Photochem. Photobiol. Sci.* 8 (2009) 1006.
- [46] G.M. Sheldrick, *SHELXS-97: Program for Crystal Structure Solution*, University of Göttingen, Germany, 1997.
- [47] G. M. Sheldrick, *SHELXL-97: Program for crystal structure refinement*; University of Göttingen, Germany, 1997.
- [48] M.J. Frisch, G.W. Trucks, H.B. Schlegel, G.E. Scuseria, M. Robb, J.R. Cheeseman, et al., *GAUSSIAN03*, Gaussian, Inc., Wallingford CT, 2004.